

# N2091S Mutation in L-type Calcium Channel Promotes Action Potential Alternans in M Cells of Human Ventricle: A Simulation Study

Yumin Shen<sup>1</sup>, Na Zhao<sup>1</sup>, Zhipeng Cai<sup>1</sup>, Chengyu Liu<sup>1</sup>, Jianqing Li<sup>1</sup>

<sup>1</sup>School of Instrument Science and Engineering, Southeast University, Nanjing, China

## Abstract

*CACNA1C-N2091S mutation has increased risk for sudden cardiac death (SCD) and action potential (AP) alternans is closely related to ventricular arrhythmias and SCD. However, the contribution of N2091S mutation on AP alternans is unidentified. This study aimed to investigate the effect of N2091S mutation on AP alternans in ventricular myocytes. N2091S mutation apparently increased L-type calcium current ( $I_{CaL}$ ), which further prolonged the AP duration and increased the  $Ca^{2+}$  concentration. Subsequently, it has been proved that N2091S mutation caused a decrease in threshold of stimulation frequency for AP alternans and wider alternans vulnerable window in midmyocardial cells (M cells). Further study demonstrated that AP alternans was induced only when increasing maximal  $I_{CaL}$  conductance ( $G_{CaL}$ ) exceeded a critical value (156.98% larger than that in WT). It produced the prolongation of AP plateau phase that led to the inhibition of inward  $I_{NCX}$  and the increase of sarcoplasmic reticulum (SR)  $Ca^{2+}$  loading. Furthermore, the resulting incomplete recovery of  $I_{CaL}$  promoted inward  $I_{NCX}$  and decreased SR  $Ca^{2+}$  loading in the next pacing cycle, consequently facilitating the genesis of  $Ca^{2+}$  cycling and AP alternans. This study demonstrated that N2091S mutation made M cells more prone to arrhythmia and the increase of  $G_{CaL}$  was the main factor for inducing alternans.*

## 1. Introduction

Since the unpredictability of sudden cardiac death (SCD) and difficulties in determining etiology, SCD becomes a significant cause of death, which is estimated to cause 5 million deaths in the world each year[1]. T-wave alternans has already been proved to be a useful marker for assessing the SCD risk clinically[2], while action potential (AP) alternans, the one of manifestations of T-wave alternans at the cellular level, is the beat-to-beat alternations in amplitude or duration of AP that is closely related to malignant ventricular arrhythmias and SCD. Numerous studies have shown that instability of voltage kinetics or  $Ca^{2+}$  handling dynamics is related to AP alternans[3]-[4].

However, under different circumstances the pathological mechanism of AP alternans is different. Since AP alternans is associated with fatal arrhythmias, it's important to explore the dominant factors that induce AP alternans.

Ion channel remodelling caused by genetic mutations may lead to AP alternans at high pacing frequency resulting in SCD in specific clinical circumstances[5]. Sutphin et al.[6] identified CACNA1C-N2091S mutation which was localized in the C-terminus of L-type calcium channel (LTCC) and confirmed that N2091S mutation caused an increased risk for SCD. Bai[7] also found that triggered activity occurred under the N2091S mutation condition at high heart rate. However, the contribution of N2091S mutation on AP alternans is unidentified. Therefore, the aim of our study is to investigate the effects of N2091S mutation on AP alternans in ventricular myocytes at cellular level by computer modelling.

## 2. Methods

The ten Tusscher et al. human ventricular myocyte model (TP06 model)[8] incorporating CaMKII regulation, updated by Bai, was used in this study. Based on the experimental data[6] and N2091S mutant ventricular myocyte model developed by Bai[7], LTCC was altered under the N2091S mutation condition, including steady-state activation  $d_{\infty}$ , steady-state voltage inactivation  $f_{\infty}$  and maximal  $I_{CaL}$  conductance  $G_{CaL}$  (see in Figure 1A). Eq. (1)[8] showed  $I_{CaL}$  was affected by  $G_{CaL}$ , voltage activation gate  $d$ , slow and fast voltage inactivation gate  $f$  and  $f_2$ , fast subspace calcium inactivation gate  $f_{cass}$ , membrane potential  $V$ ,  $Ca^{2+}$  concentration in subspace  $[Ca^{2+}]_{ss}$  and extracellular  $Ca^{2+}$  concentration  $[Ca^{2+}]_o$ .

$$I_{CaL} = G_{CaL} d f f_2 f_{cass} 4 \frac{(V-15)F^2}{RT} \times \frac{0.25[Ca^{2+}]_{ss} e^{2(V-15)F/RT} - [Ca^{2+}]_o}{e^{2(V-15)F/RT} - 1} \quad (1)$$

Boltzmann transport equation is generally used to fit steady-state activation and inactivation curves, hence  $d_{\infty}$  and  $f_{\infty}$  can be described as the followings[8]:

Table 1. Comparison of biological experiment data (E) and model data (M) under the WT and N2091S mutation conditions.

	$V_{d,1/2}$ (mV)	$V_{f,1/2}$ (mV)	$k_d$	$k_f$	$G_{CaL}$ (mm <sup>3</sup> /(ms· $\mu$ F))
WT (E)	17.1±1.1	-23.3±1.03	6.6±0.5	7.35±0.61	0.00003980
WT (M)	17.1	-23.3	6.6	7.35	
N2091S (E)	13.7±1.2	-23.3±2.31	6.2±0.4	9.09±1.32	0.00006885
N2091S (M)	13.7	-23.3	6.2	9.09	

$$d_{\infty} = \frac{1}{1 + \exp\left[\frac{(V_{d,1/2} - V_m)}{k_d}\right]} \quad (2)$$

$$f_{\infty} = \frac{1}{1 + \exp\left[\frac{(V_m - V_{f,1/2})}{k_f}\right]} \quad (3)$$

Where  $V_{d,1/2}$  and  $V_{f,1/2}$  are the membrane potentials at 50% activation and inactivation respectively,  $k_d$  and  $k_f$  are the slopes of corresponding curves at 50% activation and inactivation respectively. These parameters related to  $d_{\infty}$ ,  $f_{\infty}$  used in the case of the wild type (WT) and N2091S mutation in the model were shown in Table 1. The corresponding values of  $G_{CaL}$  in the WT and N2091S mutation type with the reference to Bai's model[7] were also listed in Table 1. Figure 1B and Figure 1C showed the simulated steady-state activation and inactivation curves under the WT and N2091S mutation conditions, which were consistent with biological experiment results[6].

High heart rate may cause alternation of contraction strength[9], hence a dynamic pacing protocol was used and action potential duration (APD) rate adaptation curves were recorded, which were determined by measuring the steady-state APD applying in 10-ms decrease to pacing cycle length (PCL) ranging from 1200 to 300ms. Simulations were run on a Windows laptop with 2.40GHz Intel Core i5-6200U CPU using a C/C++ code.

### 3. Results

#### 3.1. Effect of N2091S Mutation on Ventricular Myocyte Electrophysiology

The electrophysiology simulations were performed in endocardial, epicardial and midmyocardial cells under the WT and N2091S mutation conditions at 1-Hz pacing frequency. Compared with the WT, N2091S mutation apparently increased  $I_{CaL}$ , which further prolonged APD, promoted inward  $Na^+/Ca^{2+}$  exchanger current ( $I_{NCX}$ ), elevated the  $Ca^{2+}$  concentration in cytoplasm ( $[Ca^{2+}]_i$ ) and sarcoplasmic reticulum ( $[Ca^{2+}]_{SR}$ ). Particularly in midmyocardial cells (M cells), early afterdepolarizations occurred (Figure 1D) and double peaks were observed in inward  $I_{NCX}$ ,  $[Ca^{2+}]_i$  and  $[Ca^{2+}]_{SR}$  (Figures 1F-1H).

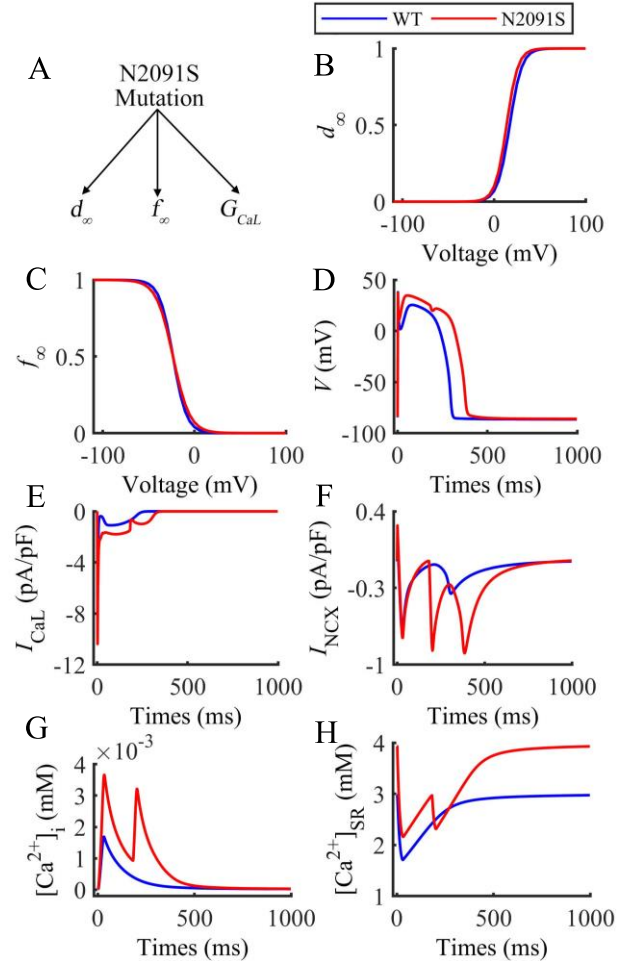


Figure 1. The effect of N2091S mutation on M cells. (A) The parameters changed by N2091S mutation. The electrophysiological variables in M cells in the case of the WT/N2091S mutation at PCL of 1000ms: (B) Steady-state activation curves, (C) Steady-state inactivation curves, (D)  $V$ , (E)  $I_{CaL}$ , (F)  $I_{NCX}$ , (G)  $[Ca^{2+}]_i$ , (H)  $[Ca^{2+}]_{SR}$ .

#### 3.2. AP Alternans Induced by N2091S Mutation in M Cells

As increasing the pacing rate, bifurcation of APD rate dependence curves occurred only in M cells under both

WT and N2091S mutation conditions, which meant APD oscillated between multiple values at the same frequency. It can be observed in Figure 2 that AP alternans occurred at PCL ranging from 570 ms to 600 ms under the WT condition and at PCL ranging from 460 ms to 640 ms and 300 ms under the N2091S mutation condition in M cells. Comparing with the WT, N2091S mutation caused a decrease in threshold of stimulation frequency for AP alternans and wider alternans vulnerable window, which made M cells more prone to arrhythmia.

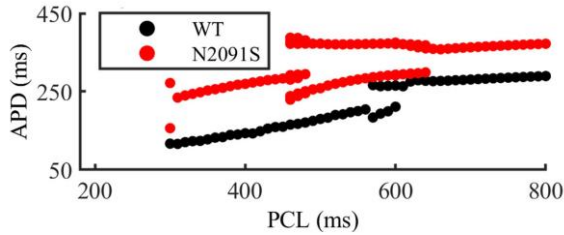


Figure 2. APD rate dependence curves of M cells under the WT and N2091S mutation conditions.

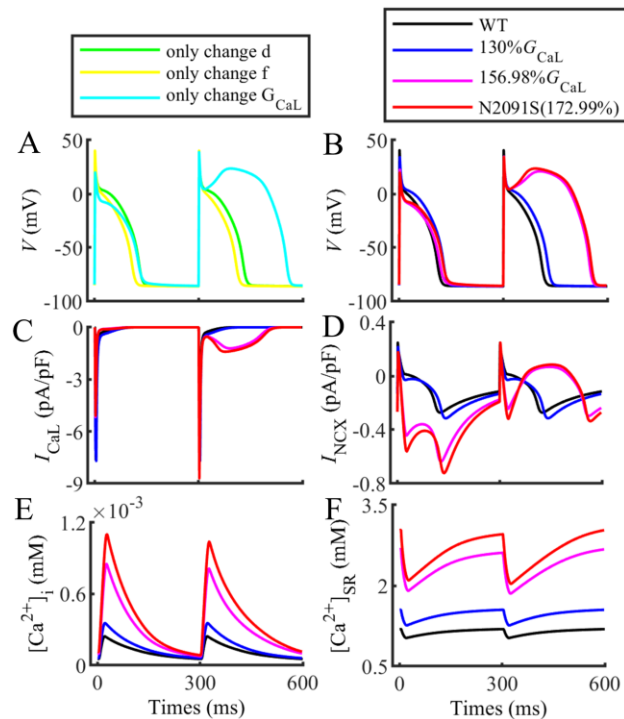


Figure 3. Effect of  $I_{CaL}$  Conductance on N2091S Mutation. (A) The action potential in M cells when changing  $d_{\infty}$ ,  $f_{\infty}$  and  $G_{CaL}$  respectively at PCL of 300ms. The electrophysiological variables in M cells when only increasing  $G_{CaL}$  at PCL of 300ms: (B)  $V$ , (C)  $I_{CaL}$ , (D)  $I_{NCX}$ , (E)  $[Ca^{2+}]_i$  and (F)  $[Ca^{2+}]_{SR}$ .

### 3.3. Effect of $I_{CaL}$ Conductance on N2091S Mutation

Since N2091S mutation affected  $I_{CaL}$  kinetics by changing LTCC gate parameters ( $d_{\infty}$  and  $f_{\infty}$ ) and  $G_{CaL}$ , these parameters were changed respectively at PCL of 300 ms and then membrane potential curves were recorded. The simulation results indicated AP alternans was induced only by increasing  $G_{CaL}$  rather than LTCC gate parameters  $d_{\infty}$  and  $f_{\infty}$  in M cells as shown in Figure 3A.  $G_{CaL}$  in the WT was set to  $0.00003980 \text{ mm}^3/(\text{ms}\cdot\mu\text{F})$ , while  $G_{CaL}$  in the N2091S mutant was set to  $0.00006885 \text{ mm}^3/(\text{ms}\cdot\mu\text{F})$ [7], 172.99% larger than it in the WT. APD gradually increased with the increase of  $G_{CaL}$  (Figure 3B) and AP alternans occurred when  $G_{CaL}$  exceeded a critical value (156.98% larger than it in the WT). Above the critical value, the larger the  $G_{CaL}$ , the greater the amplitude of alternans especially for  $I_{CaL}$  and  $I_{NCX}$  (Figures 3C-3D). In addition,  $Ca^{2+}$  concentration in cytoplasm and SR ( $[Ca^{2+}]_i$  and  $[Ca^{2+}]_{SR}$ ) were elevated greatly (Figures 3E-3F) as  $G_{CaL}$  increased.

## 4. Discussion

In this study, the effect of N2091S mutation on ventricular myocyte electrophysiology and the underlying mechanism of N2091S mutation leading to arrhythmias in M cells were investigated using TP06 model[8] with CaMKII regulation added by Bai[7] at cellular level. The novelty of this paper is to clarify the contribution of N2091S mutation on AP alternans. Our major findings follow: (i) N2091S mutation raised the risk of arrhythmias in M cells by decreasing threshold of stimulation frequency for AP alternans and widening alternans vulnerable window. (ii) The increase of  $G_{CaL}$  was the main factor that made M cells more prone to AP alternans. (iii) The simulation results related to  $Ca^{2+}$  cycling revealed the whole process of alternans induced by N2091S mutation, which was described in detail below.

For better comparison, the period with larger APD was referred to the odd period and the period with smaller APD was referred to the even period. Meanwhile, the curves of each variable in the odd and even periods at PCL of 300 ms were plotted on the same axis (Figure 4A). N2091S mutation increased  $I_{CaL}$  current resulting in prolonged AP plateau phase and APD. Prolongation of the AP plateau phase inhibited inward  $I_{NCX}$ , which made  $[Ca^{2+}]_i$  decline slowly. In late stage of repolarization, the high level of  $[Ca^{2+}]_i$  enhanced SR  $Ca^{2+}$  uptake flux ( $J_{up}$ ) and more  $Ca^{2+}$  was loaded to SR making initial  $[Ca^{2+}]_{SR}$  higher in the even period (red curves). Since SR acts as the main  $Ca^{2+}$  storage organelle[3], SR  $Ca^{2+}$  content determines systolic  $Ca^{2+}$  in cytoplasm, so that increased SR  $Ca^{2+}$  loading determined a great amplitude of  $Ca_i$  transient (cytosolic  $Ca^{2+}$  transient) in the next period. Due to the short diastolic interval, incomplete recovery of  $I_{CaL}$  caused decreased  $I_{CaL}$ , which subsequently shortened AP plateau phase and APD. This promoted inward  $I_{NCX}$  allowing a faster decline in  $[Ca^{2+}]_i$ , which later on weakened  $J_{up}$  during late stage of

repolarization. Hence SR  $\text{Ca}^{2+}$  loading was decreased determining a small amplitude of  $\text{Ca}_i$  transient in next period (the odd period). Therefore, AP alternans and  $\text{Ca}_i$  transient alternans repeated indefinitely, which was described as the flow diagram in Figure 4B.

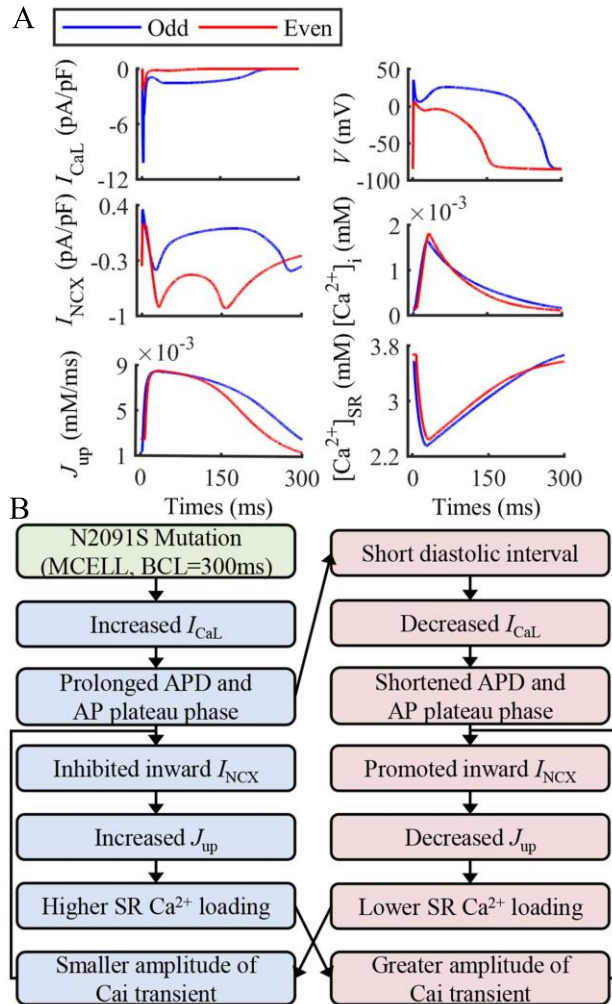


Figure 4. Internal mechanism of alternans caused by N2091S mutation. (A) Comparison of electrophysiological variables in the odd/even period at PCL of 300ms. (B) Flow chart of the alternans mechanism.

In this study, the simulation results were obviously consistent with negative  $\text{Ca}_i \rightarrow V$  coupling, which meant a larger APD was accompanied with a smaller  $\text{Ca}_i$  transient[4]. During the whole process of alternation, voltage kinetics and  $\text{Ca}^{2+}$  handling dynamics were coupled via  $I_{\text{NCX}}$  acting as an important intermediate to connect  $\text{Ca}^{2+}$  in cytoplasm and SR. In addition, it has been proved that  $\text{Ca}_i$  alternans depends on alternation of  $\text{Ca}^{2+}$  content in SR[10], similarly in this study SR  $\text{Ca}^{2+}$  loading played a crucial role in  $\text{Ca}_i$  alternans, which was reflected in the fact that the level of SR  $\text{Ca}^{2+}$  determined the amplitude of  $\text{Ca}_i$  transient in the next period.

## Acknowledgments

National Natural Science Foundation of China (62001105).

## References

- [1] J. Isbister and C. Semsarian, "Sudden Cardiac Death: An Update," *Internal medicine journal*, vol. 49, no. 07, pp. 826-833, Jul. 2019.
- [2] M.J. Cutler and D. S. Rosenbaum, "Explaining the Clinical Manifestations of T Wave Alternans in Patients at Risk for Sudden Cardiac Death," *Heart rhythm*, vol. 06, no. 03, pp. S22-S28, Mar. 2009.
- [3] Y.L. Zang and L. Xia, "Cellular Mechanism of Cardiac Alternans: An Unresolved Chicken or Egg Problem," *Journal of Zhejiang University SCIENCE B*, vol. 15, no. 03, pp. 201-211, Mar. 2014.
- [4] J.N. Weiss, A. Karma, Y. Shiferaw, P.S. Chen, A. Garfinkel and Z. Qu, "From Pulsus to Pulseless: The Saga of Cardiac Alternans," *Circulation research*, vol. 98, no. 10, pp. 1244-1253, May 2006.
- [5] U. Schweigmann, P. Biliczki, R.J. Ramirez, C. Marschall, I. Takac and R.P. Brandes et al., "Elevated Heart Rate Triggers Action Potential Alternans and Sudden Death. Translational Study of a Homozygous KCNH2 Mutation," *PLoS ONE*, vol. 09, no. 08, pp. e103150, Aug. 2014.
- [6] B.S. Sutphin, N.J. Boczek, H. Barajas-Martinez, D. Hu, D. Ye, D.J. Tester, C. Antzelevitch and M.J. Ackerman, "Molecular and Functional Characterization of Rare CACNA1C Variants in Sudden Unexplained Death in the Young," *Congenital Heart Disease*, vol. 11, no. 06, pp. 683-692, May 2016.
- [7] J. Bai, Y. Lu, T. Song, K. Wang and H. Zhang, "In Silico Investigation of the CACNA1C N2091S Mutation in Timothy Syndrome," *2019 Computing in Cardiology (CinC)*, 2019, pp. Page 1-Page 4, doi: 10.23919/CinC49843.2019.9005763.
- [8] K. Tusscher and A. V. Panfilov, "Alternans and Spiral Breakup in a Human Ventricular Tissue Model," *American journal of physiology Heart and circulatory physiology*, vol. 291, no. 03, pp. H1088-1100, Mar. 2006.
- [9] I.R. Cantalapiedra, E. Alvarez-Lacalle, A. Penaranda and B. Echebarria, "Minimal Model for Calcium Alternans Due to SR Release Refractoriness," *Chaos*, vol. 27, no. 09, pp. 093928, Mar. 2017.
- [10] M.E. Diaz, S.C. O'Neill and D.A. Eisner, "Sarcoplasmic Reticulum Calcium Content Fluctuation Is the Key to Cardiac Alternans," *Circulation Research: Journal of The American Heart Association*, vol. 94, no. 05, pp. 650-656, Jan. 2004.

Address for correspondence:

Chengyu Liu, PhD; Jianqing Li, PhD  
 School of Instrument Science and Engineering  
 Southeast University, China  
 E-mail: chengyu@seu.edu.cn; lj@seu.edu.cn